

Surface trapping and leakage of low-frequency g modes in rotating early-type stars – II. Global analysis

R. H. D. Townsend[★]

Department of Physics & Astronomy, University College London, Gower Street, London WC1E 6BT

Accepted 2000 July 7. Received 2000 July 5; in original form 2000 May 8

ABSTRACT

A global analysis of the surface trapping of low-frequency non-radial g modes in rotating early-type stars is undertaken within the Cowling, adiabatic and traditional approximations. The dimensionless pulsation equations governing these modes are reviewed, and the boundary conditions necessary for solution of the equations are considered; in particular, an outer mechanical boundary condition, which does not enforce complete wave trapping at the stellar surface, is derived and discussed in detail. The pulsation equations are solved for a $7-M_{\odot}$ model star over a range of rotation rates, using a numerical approach.

The results of the calculations confirm the findings of the preceding paper in the series: modes with eigenfrequencies below a cut-off cannot be fully trapped within the star, and exhibit leakage in the form of outwardly propagating waves at the surface. The damping rates resulting from leakage are calculated for such ‘virtual’ modes, and found to be appreciably larger than typical growth rates associated with opacity-driven pulsation. Furthermore, it is demonstrated that the surface perturbations generated by virtual modes are significantly changed from those caused by fully trapped modes; the latter result suggests differences in the line-profile variations exhibited by these two types of mode.

The findings are discussed in the context of the 53 Per, SPB and pulsating Be classes of variable star. Whilst wave leakage will probably not occur for overstable g modes in the 53 Per and slowly rotating SPB stars, the adoption of the new outer mechanical boundary condition may still affect the pulsational stability of these systems. Wave leakage for overstable modes remains a possibility in Be stars and the more rapidly rotating SPB stars.

Key words: waves – stars: early-type – stars: emission-line, Be – stars: oscillations – stars: rotation.

1 INTRODUCTION

The first paper in this series (Townsend 2000, hereinafter Paper I) presented a qualitative analysis of the surface trapping and leakage of low-frequency g modes in rotating early (types O and B) stars. This analysis was based around a dispersion relation for wave propagation throughout the star, derived from a local solution of the pulsation equations under the Cowling (1941) and adiabatic approximations. The influence of rotation on the wave propagation was treated via the adoption of the ‘traditional approximation’ (Eckart 1960), appropriate for low-frequency modes in moderately rotating stars. It was found that modes with frequencies ω below a trapping cut-off ω_t would leak from the star owing to the absence of a completely reflective boundary at the stellar surface; this cut-off depends, amongst other things, on the angular velocity of

rotation. These so-called virtual modes, whilst decaying in amplitude with time, exhibit discrete frequencies, for reasons which will be discussed subsequently.

The present work places the topics discussed in the preceding paper on a more quantitative footing, through solution of the pulsation equations, with appropriate boundary conditions, at a global level. The motivation for such an undertaking is threefold: first, to confirm the validity of results obtained in Paper I, secondly, to place constraints on the properties of the virtual modes mentioned above, and lastly, to lay the foundations for the following paper in this series, which will investigate the line-profile variations generated by virtual-mode excitation. The following section reviews the appropriate pulsation equations and boundary conditions; the method adopted for numerical solution of the equations is described in Section 3, whilst the results from corresponding calculations are presented in Section 4. The findings are then discussed in Section 5, and summarized in Section 6.

[★] E-mail: rhdt@star.ucl.ac.uk

2 PULSATION EQUATIONS

Within the traditional approximation adopted throughout Paper I, the horizontal component of the angular frequency vector of rotation, $\mathbf{\Omega}$, is neglected. In combination with the Cowling and adiabatic approximations, where the perturbations to the gravitational potential and specific entropy, respectively, are suppressed, the traditional approximation considerably reduces the complexity of linear pulsation theory in rotating stars, by rendering the governing equations separable in spherical polar coordinates (r, θ, ϕ) . The angular dependence of solutions is described by $\Theta_l^m(\mu; \nu) \exp(im\phi)$, where $\mu \equiv \cos \theta$ and $\Theta_l^m(\mu; \nu)$ is a Hough function (Bildsten, Ushomirsky & Cutler 1996; Lee & Saio 1997), whilst the radial dependence is found from solving a pair of coupled first-order differential equations. These equations contain coefficients which depend on the underlying structure of the pulsating star, and require a numerical approach for solution. The form of the equations presented in Paper I is not suitable for such calculations, since the coefficients appearing therein vary by many orders of magnitude throughout a typical star; accordingly, a more-appropriate dimensionless formulation is reviewed below.

The system of radial-component pulsation equations is effectively second order in nature, and general solutions therefore contain two arbitrary constants of integration. These constants, plus regularity conditions required to ensure that solutions are physically realistic, lead to boundary conditions applicable to the system at the origin and stellar surface. As will be demonstrated, these boundary conditions, discussed in the latter parts of this section, are of paramount importance when issues of wave trapping and leakage are considered.

2.1 Dimensionless formulation

Whilst there exists a plethora of possible formulations of the pulsation equations from which to choose, that introduced by Dziembowski (1971) has proven to be very popular, and is adopted herein. The radial fluid displacement ξ_r and Eulerian pressure perturbation p' are expressed in terms of dependent variables y_1 and y_2 ,

$$y_1(r) = \frac{\xi_r}{r}, \quad y_2(r) = \frac{p'}{\rho g r}, \quad (1)$$

where, as in Paper I, ρ and g are the local equilibrium values of the density and gravitational acceleration, respectively. Note that the expression for y_2 is a reduced form of that originally used by Dziembowski (1971), since Φ' , the perturbation to the gravitational potential, is set to zero in accordance with the Cowling approximation. With these definitions, the equations governing y_1 and y_2 in a rotating star, subject to the traditional approximation, may be written in the canonical form

$$x \frac{dy_1}{dx} = (V_g - 3)y_1 + \left(\frac{\lambda_{lm}}{c_1 \hat{\omega}^2} - V_g \right) y_2, \quad (2)$$

$$x \frac{dy_2}{dx} = (c_1 \hat{\omega}^2 - A^*)y_1 + (1 + A^* - U)y_2 \quad (3)$$

(see, e.g. Lee & Saio 1989). Here, λ_{lm} is the eigenvalue associated with the appropriate Hough function $\Theta_l^m(\mu, \nu)$; as discussed in Paper I, this eigenvalue is a measure of the effective wavenumber of solutions in the transverse (horizontal) direction. The influence of the Coriolis force on pulsation is reflected in the variation of λ_{lm} with rotation parameter $\nu \equiv 2\Omega/\omega$, where $\mathbf{\Omega} \equiv |\mathbf{\Omega}|$ is the

angular frequency of rotation. The independent variable x and dimensionless pulsation frequency $\hat{\omega}$ are defined through

$$x = \frac{r}{R}, \quad \hat{\omega}^2 = \frac{\omega^2 R^3}{GM}, \quad (4)$$

where M , R and G are the stellar mass, stellar radius and gravitational constant, respectively. The other coefficients in equations (2) and (3) are defined as

$$V_g = \frac{V}{\Gamma_1} = -\frac{1}{\Gamma_1} \frac{d \ln p}{d \ln r} = \frac{gr}{c_s^2}, \quad c_1 = \frac{r^3 M}{R^3 M_r},$$

$$U = \frac{d \ln M_r}{d \ln r} = \frac{4\pi \rho r^3}{M_r}, \quad A^* = \frac{r N^2}{g}, \quad (5)$$

where M_r , c_s and N are the mass interior to radius r , adiabatic sound speed and Brunt–Väisälä frequency, respectively, and Γ_1 is the first adiabatic exponent. The above four expressions are identical to those used throughout Unno et al. (1989).

2.2 Boundary conditions

The boundary conditions applicable to the eigenfunctions $y_{1,2}$ may be derived by considering the limiting behaviour of the dimensionless pulsation equations (2) and (3) at the origin and at the stellar surface. The former boundary presents some difficulty in the case with rotation, since the assumption that radial fluid displacements are dominated by horizontal ones, required within the traditional approximation (e.g. Lee & Saio 1997), becomes inappropriate as the centre of the star is approached. However, the core regions of early-type stars are unstable against convection ($N^2 < 0$), and g modes will be evanescent in character throughout; therefore, the formal breakdown of the traditional approximation should not lead to significant errors.

At the centre of the star, the limiting values

$$\left. \begin{array}{l} V_g \rightarrow 0 \\ U \rightarrow 3 \\ A^* \rightarrow 0 \end{array} \right\} \text{ as } x \rightarrow 0 \quad (6)$$

may be substituted into (2) and (3) to yield the differential equations pertaining to the origin,

$$x \frac{dy_1}{dx} = -3y_1 + \frac{\lambda_{lm}}{c_1 \hat{\omega}^2} y_2, \quad (7)$$

$$x \frac{dy_2}{dx} = c_1 \hat{\omega}^2 y_1 - y_2. \quad (8)$$

At $x=0$, c_1 approaches a limiting value given by the ratio between the central and mean densities of the star; therefore, the above two equations may be regarded as having constant coefficients. Solutions of the form $y_{1,2} \sim x^\alpha$ then lead to a characteristic equation for the exponent α , with roots given by

$$\alpha = \begin{cases} \tilde{l} - 2, \\ -(\tilde{l} + 3); \end{cases} \quad (9)$$

here, \tilde{l} is a rotationally modified equivalent of the harmonic degree l , and is defined through

$$\tilde{l} = \frac{2\lambda_{lm}}{1 + \sqrt{1 + 4\lambda_{lm}}}, \quad (10)$$

so that $\tilde{l}(\tilde{l} + 1) \equiv \lambda_{lm}$ and $\tilde{l} \rightarrow l$ in the limit of no rotation ($\nu = 0$).

The second root given in (9) must be discarded, since, for $\tilde{l} > 0$, it describes solutions which are singular at the origin. The other root leads to solutions which, when substituted into equations (7) and (8), must satisfy the relation

$$c_1 \tilde{\omega}^2 y_1 - \tilde{l} y_2 = 0; \quad (11)$$

this is the inner boundary condition, and, in essence, is identical to that applicable to a non-rotating star (e.g. Unno et al. 1989) when the equivalence between \tilde{l} and l is understood.

The requirement that both ξ_r and p' are finite at the origin indicates that acceptable solutions must satisfy $\alpha \geq -1$, or, equivalently, $\tilde{l} \geq 1$. For a given l , the eigenvalue λ_{lm} of the prograde sectoral ($m = -l$) mode is the smallest in the asymptotic limit $\nu \gg 1$, approaching the value $m^2 = l^2$ (Bildsten et al. 1996). Whilst no formal proof is offered, experience suggests that λ_{lm} exceeds this limiting value for all other values of m and ν . Therefore, it would appear that the requirement that $\tilde{l} \geq 1$ can only be guaranteed for $l \geq 2$: the boundary condition (11) should be treated with extreme caution for $l = 1$ modes, and, of course, is not appropriate at all for $l = 0$ (radial) modes.

The linear nature of the pulsation problem (at small physical amplitudes) means that solutions scaled by some arbitrary constant will still satisfy the pulsation equations (2) and (3); therefore, it is necessary to adopt some normalization convention. An appropriate choice is that

$$y_1 = 1 \quad (12)$$

at the outer boundary, which is convenient for numerical calculations since solutions will have an order of magnitude of unity. Once solutions have been found, they can, of course, be re-scaled to more physically realistic amplitudes.

The derivation of the outer mechanical boundary condition, which completes the triplet required for solution of the pulsation equations, is somewhat more ambiguous than those for the other two conditions (11) and (12). One possible approach (e.g. Glatzel & Gautschy 1992) is to require that the fractional Lagrangian pressure perturbation $\delta p/p$ vanishes at the stellar surface; since

$$\delta p = pV(y_2 - y_1) \quad (13)$$

in the Cowling approximation, this is equivalent to

$$y_1 - y_2 = 0, \quad (14)$$

the so-called ‘zero boundary condition’. A less stringent formulation, originally introduced by Dziembowski (1971), and subsequently adopted by a number of authors (e.g. Osaki & Hansen 1973; Dziembowski, Moskalik & Pamyatnykh 1993), requires that the *gradient* of $\delta p/p$ vanishes at the surface. In the context of a rotating star, within the traditional approximation, the resulting boundary condition is given by

$$\left[1 + \frac{1}{V} \left(\frac{\lambda_{lm}}{\tilde{\omega}^2} - 4 - \tilde{\omega}^2 \right) \right] y_1 - y_2 = 0, \quad (15)$$

which is derived in a straightforward manner from Dziembowski’s (1971) non-rotating expression by replacing $l(l+1)$ with λ_{lm} . Strictly speaking, this boundary condition is only valid when $\tilde{\omega}^2/V$ and $\lambda_{lm}/(\tilde{\omega}^2 V)$ are much smaller than unity; similar requirements were stipulated by Dziembowski for the equivalent non-rotating case.

At low frequencies, the latter of these two requirements can break down, since $\tilde{\omega}^2$ is small and λ_{lm} can become large, owing to the confinement of modes within the equatorial waveguide

(Paper I); therefore, a more general formulation of the outer mechanical boundary condition must be developed. Ando & Osaki (1975), in considering the solar pulsation problem, used an approach which may easily be adapted to include the influence of rotation (note that their calculations were, in general, non-adiabatic, but they used the adiabatic approximation in deriving the outer boundary condition, so their method remains applicable). The derivation follows the same procedure as that used to find the inner boundary condition (11): at the surface, the limiting values

$$\left. \begin{array}{l} U \rightarrow 0 \\ c_1 \rightarrow 1 \end{array} \right\} \text{ as } x \rightarrow 1 \quad (16)$$

lead to the equations

$$x \frac{dy_1}{dx} = (V_g - 3)y_1 + \left(\frac{\lambda_{lm}}{\tilde{\omega}^2} - V_g \right) y_2, \quad (17)$$

$$x \frac{dy_2}{dx} = (\tilde{\omega}^2 - A^*) + (1 + A^*)y_2. \quad (18)$$

As before, the coefficients in these equations are assumed to be constant, and solutions of the form $y_{1,2} \sim x^\beta$ give a characteristic equation with roots

$$\beta = \frac{1}{2} [(V_g + A^* - 2) \pm \psi], \quad (19)$$

where the ‘propagation discriminant’ ψ is defined by

$$\psi = \left[(A^* - V_g + 4)^2 + 4 \left(\frac{\lambda_{lm}}{\tilde{\omega}^2} - V_g \right) (\tilde{\omega}^2 - A^*) \right]^{1/2}. \quad (20)$$

The ‘leaky’ outer mechanical boundary condition is then found as

$$(A^* - V_g + 4 \pm \psi)y_1 - 2 \left(\frac{\lambda_{lm}}{\tilde{\omega}^2} - V_g \right) y_2 = 0, \quad (21)$$

which, as expected, is equivalent to the expression found by Ando & Osaki (1975) in the non-rotating case.

It is evident from inspection of (19) and (20) that β in the leaky boundary condition (21) can be complex, even when $\tilde{\omega}$ is purely real. In such cases, global solution of the pulsation equations (2) and (3) will lead to eigenfunctions and eigenfrequencies which, too, are complex. Near the stellar surface, these eigenfunctions will vary as

$$y_{1,2} \sim \exp[(\beta_R + i\beta_I) \ln x] \exp[i(\omega_R + i\omega_I)t], \quad (22)$$

where, henceforth, the subscripts ‘R’ and ‘I’ denote real and imaginary parts, respectively. Defining $z \equiv x - 1$ as the normalized distance above the stellar surface, this expression is approximated at small z by

$$y_{1,2} \sim \exp(\beta_R z - \omega_I t) \exp[i(\beta_I z + \omega_R t)], \quad (23)$$

which can be recognized as a canonical form for propagating waves which grow or decay exponentially, in both space and time. Therefore, such solutions correspond to the leaking virtual modes introduced in Paper I.

To investigate the conditions under which virtual modes will arise, it is pertinent to examine the dependence of the propagation discriminant ψ on $\tilde{\omega}$; accordingly, Fig. 1 shows ψ_R and ψ_I over the region of the $(\tilde{\omega}_R, \tilde{\omega}_I)$ complex plane which corresponds to g modes (i.e. $\tilde{\omega}_R \lesssim 1$). In calculating ψ , λ_{lm} was assigned a value of 20, which corresponds to a harmonic degree $l = 4$ in the non-rotating case; furthermore, the values $V_g = 919$ and $A^* = 287$ were adopted from the outer grid point of the 7- M_\odot model star

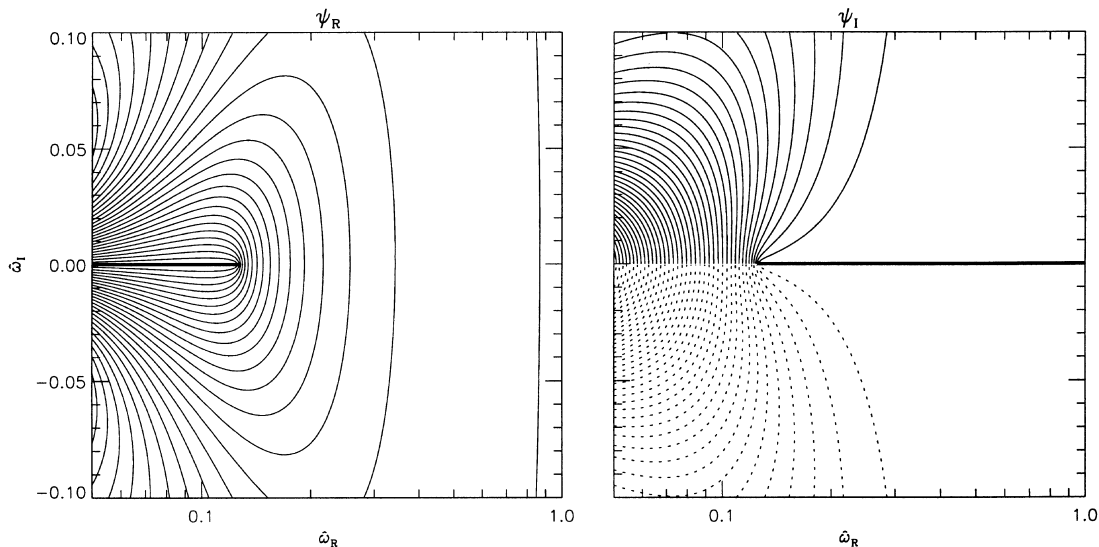


Figure 1. ψ_R and ψ_I , the real and imaginary parts, respectively, of the propagation discriminant ψ , plotted over the $(\hat{\omega}_R, \hat{\omega}_I)$ complex plane for $V_g = 919$, $A^* = 287$ and $\lambda_{lm} = 20$. Solid (dotted) lines show contours of constant positive (negative) $\psi_{R,I}$, spaced at intervals $\Delta\psi = 70$, whilst thick solid lines indicate where $\psi_{R,I} = 0$.

considered throughout Section 4. The branch cut along the negative real axis was used in evaluating the square root in expression (20), such that $\psi_R \geq 0$ for all $\hat{\omega}$; this convention accounts for the discontinuity in ψ_I across the $\hat{\omega}_I = 0$ axis, evident in the figure for $\hat{\omega}_R \leq 0.126$.

Following Unno et al. (1989), two dimensionless frequencies, $\hat{\omega}_{c_1}$ and $\hat{\omega}_{c_2}$, are introduced as the (real) roots of the equation $\psi = 0$ (and, hence, the branch points of ψ), with $\hat{\omega}_{c_2} > \hat{\omega}_{c_1}$. It is evident from inspection of Fig. 1 that the point $\hat{\omega}_R \approx 0.126$ on the $\hat{\omega}_I = 0$ axis, where ψ is identically zero, may be identified with $\hat{\omega}_{c_1}$; a corresponding point at $\hat{\omega}_R \approx 19.9$ (not shown in the figure) can similarly be identified with $\hat{\omega}_{c_2}$. When $\hat{\omega}_{c_1} \leq \hat{\omega}_R \leq \hat{\omega}_{c_2}$, solutions of the pulsation equations (2) and (3) with purely real eigenfunctions and eigenfrequencies exist; these solutions, which all lie on the $\hat{\omega}_I = 0$ axis in the figure, correspond to complete wave trapping within the star. In such situations, the sign of ψ in the leaky boundary condition (21) must be taken to be negative; this is to ensure that the mechanical energy density \mathcal{E} owing to pulsation, given by (e.g. Unno et al. 1989; Wang, Ulrich & Coroniti 1995)

$$\mathcal{E} \sim \exp(\pm\psi_R z - 2\omega_I t), \quad (24)$$

decays as z increases above the surface.

When $\hat{\omega}_R < \hat{\omega}_{c_1}$, no purely real values of ψ exist in the $(\hat{\omega}_R, \hat{\omega}_I)$ plane, and wave leakage of the form described by (23) must occur; therefore, $\hat{\omega}_{c_1}$ may be identified as a dimensionless form of the trapping cut-off frequency ω_t introduced in Paper I. Note that the definitions of these two quantities are not completely equivalent, owing to the presence of the leading $(A^* - V_g + 4)^2$ term in definition (20) of ψ , which arises from differences in the approximations adopted in the derivations. As before, the sign of ψ in the outer boundary condition must be chosen to ensure that solutions are physically acceptable; in the present case, the requirement is that leaking waves have an upward (positive) radial group velocity, and therefore transport energy outwards through the stellar surface. Using the well-known result that the radial group and phase velocities of g modes are opposite in direction (e.g. Gill 1982; Unno et al. 1989), it is evident that the sign of ψ

must be chosen such that the phase velocity is *negative*; this is equivalent to the requirement that β_I be positive, since waves described by equation (23) have a phase velocity $-\omega_R/\beta_I$, and the convention that ω_R is positive is adopted throughout.

Once solutions to the pulsation equations are calculated (Section 4), it is found that ω_I is invariably greater than zero when leakage occurs; this result is to be expected, since the amplitude of virtual modes decays with time to compensate for the outward loss of mechanical energy through the stellar surface. Inspection of Fig. 1 shows that the choice of the plus sign in the boundary condition (21) will then ensure that β_I is positive, as required above. However, a corollary of such a choice is that the mechanical energy density \mathcal{E} will diverge with increasing distance above the stellar surface (see equation 24), a seemingly unphysical result.

It transpires that this behaviour is, in fact, perfectly reasonable. If the leakage is viewed as a continuous stream of spatially localized wave groups, then, at some epoch t_0 , the mechanical energy in regions above the surface is associated with those wave groups which leaked from the star prior to t_0 . Let $\langle F_W(t) \rangle$ be the instantaneous mechanical energy flux through the stellar surface owing to leakage; then this quantity, being proportional to \mathcal{E} when the group velocity is time independent, as is the case in the linear approximation, will obey the relation

$$\langle F_W \rangle(t) = \langle F_W \rangle(t_0) \exp[2\omega_I(t_0 - t)], \quad (25)$$

where $\langle \rangle$ denotes the time-average over one pulsation cycle. With $\omega_I > 0$, it is evident that $\langle F_W \rangle(t) > \langle F_W \rangle(t_0)$ for all $t < t_0$, and therefore that those wave groups emitted prior to the epoch contain more energy than those being emitted at t_0 itself. The outward divergence of \mathcal{E} found previously then follows from the fact that $(t_0 - t)$ is a monotonically increasing function of the distance of a given group above the surface. Note that the total space-integrated mechanical wave energy will be infinite, which is inconvenient but by no means fatal, and arises from treating the leakage in Fourier space, rather than as an initial-value problem. Using the latter approach, Wang et al. (1995), in considering wave propagation in an isothermal atmosphere, demonstrated that \mathcal{E} will

diverge outwards for upwardly propagating g modes, in accordance with the results presented herein, but will vanish above some (outwardly moving) radius, to give a finite total wave energy.

2.3 The steady-wave approximation

A complication arises in the adoption of the traditional approximation for the virtual modes, whose eigenfrequencies are complex. This may most easily be appreciated by considering the infinite-dimension coupling matrix \mathbf{W} , introduced by Lee & Saio (1987a), whose eigenvalues are λ_{lm} , and whose eigenvectors \mathbf{b} give the coefficients in the representation of the Hough functions $\Theta_l^m(\mu; \nu)$ as a series expansion of associated Legendre polynomials $P_l^m(\mu)$. The inverse matrix \mathbf{W}^{-1} is symmetric and tridiagonal, with every non-zero element exhibiting some dependence on the rotation parameter ν (Lee & Saio 1987a; Townsend 1997a). In situations where ν is real, it is trivial to demonstrate that \mathbf{W} is Hermitian, and, therefore, that both λ_{lm} and \mathbf{b} are real. Furthermore, since the eigenvalues λ_{lm} are non-degenerate in such cases (Townsend 1997a), the eigenvectors \mathbf{b} form a complete orthogonal vector basis, and the Hough functions are orthogonal too.

These useful properties are, unfortunately, lost when ν becomes complex (i.e. for $\omega_1 \neq 0$): \mathbf{W} is symmetric but not Hermitian, owing to the presence of terms in ν on the leading diagonal of \mathbf{W}^{-1} , and both λ_{lm} and \mathbf{b} are complex also. Indeed, \mathbf{W} is not even normal (i.e. $\mathbf{W}^\dagger \mathbf{W} \neq \mathbf{W} \mathbf{W}^\dagger$, where \dagger denotes the Hermitian conjugate), and thus cannot be guaranteed to possess eigenvectors which are orthogonal or complete (Press et al. 1992). As a consequence, the Hough functions cease to be orthonormal, and can no longer serve as the angular basis functions for pulsation in rotating stars. This same result can be obtained by noting that the differential operator \mathcal{L}_ν , occurring in Laplace's tidal equation (Lee & Saio 1997), of which the Hough functions are the eigensolutions, is only self-adjoint when ν is real.

The physical reason for these difficulties lies in the decay of virtual modes with time. As Ando (1983) points out, fluid-particle trajectories are symmetric over a whole cycle for pulsation which is both adiabatic and steady, but become asymmetric when *either* of these conditions are relaxed. In the present case, such an asymmetry arises from the net loss of mechanical energy and angular momentum by fluid particles over a cycle, compensating for the outward leakage of these quantities through the stellar surface. Therefore, whilst both energy and angular momentum are conserved at a global level, they are *not* at a local level, and it is this local breakdown of conservation laws which leads to the problems within the traditional approximation.

Fortunately, all is not lost. When $\omega_1 \ll \omega_R$, \mathbf{W} will be 'almost' Hermitian (i.e. $\mathbf{W} - \mathbf{W}^\dagger \approx \mathbf{0}$). In such cases, it seems reasonable to neglect ω_1 in evaluating ν (so that, by definition, $\nu = 2\Omega/\omega_R$), leading to a purely real \mathbf{W} and therefore obviating the problems. Physically, this approach corresponds to enforcing local conservation laws, at the expense of violating global ones, by ensuring that particle trajectories are steady; however, for suitably small ω_1 , the departure from global conservation will be negligible, and can be disregarded. As will be demonstrated in Section 4.3, the condition $\omega_1 \ll \omega_R$ is met for all modes considered, and the adoption of this 'steady-wave' approximation appears to be valid.

3 NUMERICAL PROCEDURE

In this section, the procedure adopted for numerical solution of the dimensionless pulsation equations (2) and (3), subject to the

appropriate boundary conditions (equations 11, 12 and 21), is discussed in detail. A direct approach at arbitrary values of Ω , whilst feasible, is computationally very expensive, owing to the implicit and non-linear functional dependence of λ_{lm} on the (initially unknown) eigenfrequencies $\hat{\omega}$. However, this dependence is itself inherently *independent* of the underlying equilibrium stellar structure; therefore, a two-stage technique suggests itself as a natural approach to the problem.

3.1 The \tilde{l} -track technique

At a formal level, the pulsation equations and boundary conditions are functions of \tilde{l} , the rotationally modified harmonic degree defined in equation (10). If, for the moment, the physical significance of the equations is disregarded, then \tilde{l} may be treated as a *free* parameter. It is reasonable to expect that, for suitably small $\Delta\tilde{l}$, solutions found at some \tilde{l} will be very similar to those at $\tilde{l} + \Delta\tilde{l}$, suggesting a relaxation method (e.g. Press et al. 1992) as an appropriate numerical approach. Such methods rely on finding some 'trial' solution, known to be close to a true solution, which is then iteratively improved until convergence is achieved. The algorithm adopted for calculating solutions as a function of \tilde{l} thus proceeds as follows: solutions are found at some initial value $\tilde{l} = \tilde{l}_s$, and are then used as trial solutions in a relaxation method at $\tilde{l} = \tilde{l}_s + \Delta\tilde{l}$. Once convergence (to some suitable tolerance) is achieved, the procedure is repeated as many times as is necessary, resulting in the tabulation of eigenfrequencies $\hat{\omega}$ as a function of $\tilde{l} \geq \tilde{l}_s$, at intervals of $\Delta\tilde{l}$. These tabulations are hereinafter referred to as ' \tilde{l} -tracks', an appellation chosen to highlight the similarity with the numerical approach for calculating stellar evolutionary tracks (e.g. Kippenhahn & Weigert 1990). It is interesting to note that Aizenman, Smeyers & Weigert (1977) have already calculated the zero-rotation equivalents to \tilde{l} -tracks, by investigating the dependence of fundamental (f) mode eigenfrequencies on non-integral values of the harmonic degree l .

In themselves, \tilde{l} -tracks are somewhat difficult to interpret, since \tilde{l} is not directly related to any of the parameters typically used to characterize pulsation, except in the non-rotating case when $\tilde{l} = l$. However, the formalism of the traditional approximation provides a means to map \tilde{l} into the rotation angular frequency Ω , a more natural parameter. Whilst this mapping depends on the particular choice of harmonic degree l and azimuthal order m , it is independent of the equilibrium stellar structure; therefore, the \tilde{l} -tracks may be viewed as a condensed representation of the pulsation characteristics of a star, at arbitrary rotation rates and for arbitrary mode parameters.

The mapping from \tilde{l} to Ω proceeds as follows: for a given l and m , the eigenvalue λ_{lm} is tabulated as a function of the rotation parameter ν using an appropriate numerical approach (e.g. Bildsten et al. 1996; Lee & Saio 1997; Townsend 1997b). These data are combined with equation (10) to calculate \tilde{l} as a function of ν . At each ordinate point in the latter tabulation, the associated abscissa value of \tilde{l} may then be used to interpolate the real part $\hat{\omega}_R$ of the eigenfrequency in the \tilde{l} -track data for each mode under consideration. Finally, the ν ordinate may be converted into a rotation angular frequency via application of the relations

$$\Omega^2 = \frac{\hat{\Omega}^2 GM}{R^3} \quad (26)$$

and

$$\hat{\Omega} = \frac{\nu \hat{\omega}_R}{2} \quad (27)$$

for each $(\nu, \hat{\omega}_R)$ pair; the former defines the dimensionless angular rotation frequency $\hat{\Omega}$, whilst the latter results from the definition of ν within the steady-wave approximation discussed in Section 2.3. The adoption of this approximation is justified in Section 4.3.

When combined with this mapping procedure, the \tilde{l} -track technique described above allows the calculation of a stellar eigenfrequency spectrum over a range of rotation rates. The technique was implemented in a FORTRAN 95 code, TAHINI, using the relaxation method presented by Unno et al. (1989), which is specifically tailored to two-point boundary eigenvalue problems; a centred differencing scheme (i.e. $\theta_i = 0.5$ in the nomenclature of Unno et al. 1989) was adopted throughout. Results generated using TAHINI are presented in Section 4; the remainder of this section is devoted to a discussion of two especially significant points regarding the implementation of the technique.

3.2 Starting solutions

As indicated previously, the \tilde{l} -track technique requires solutions at some initial value $\tilde{l} = \tilde{l}_s$ of the rotationally modified harmonic degree. These initial solutions are found by TAHINI using a procedure based on the root-finding method of Castor (1971) and Osaki & Hansen (1973). The leaky outer mechanical boundary condition is set aside, so that the pulsation equations can be solved using the relaxation method from arbitrary trial solutions and at arbitrary $\hat{\omega}$. The discriminant

$$D(\hat{\omega}) = \frac{D_1}{D_0} \quad (28)$$

is then calculated, where

$$D_1 = \left[(A^* - V_g + 4 \pm \psi)y_1 - 2 \left(\frac{\lambda_{lm}}{\hat{\omega}^2} - V_g \right) y_2 \right]_{x=1} \quad (29)$$

is the numerical value of the left-hand side of the leaky boundary condition (21) and

$$D_0 = [y_1 + y_2]_{x=0} \quad (30)$$

is a term included to ensure that $D(\hat{\omega})$ remains finite even when y_1 or y_2 diverge at the surface (see Unno et al. 1989). This term is guaranteed to be non-zero for all $\hat{\omega}_R \neq 0$ and $y_1 \neq 0$; the former requirement is satisfied for all pulsation modes other than the imaginary- $\hat{\omega}$ g^- convective modes (Aizenman & Smeyers 1977), whilst the latter holds via the normalization condition (12). When the discriminant $D(\hat{\omega})$ is zero, the excluded leaky boundary condition (21) is satisfied; therefore, the roots of $D(\hat{\omega})$ are the eigenfrequencies of the star, and are used by TAHINI, in tandem with the corresponding eigenfunctions, as initial solutions at $\tilde{l} = \tilde{l}_s$.

When complete wave trapping occurs, the roots of the discriminant $D(\hat{\omega})$ are located along the $\hat{\omega}_R$ -axis, and the root-finding problem is one-dimensional and trivial (e.g. Osaki & Hansen 1973). However, whenever leakage arises, the roots lie somewhere in the complex- $\hat{\omega}$ plane, and are somewhat more difficult to locate. The contour-integral method introduced by Dziembowski (1977) and Shibahashi & Osaki (1981) is one possible means of isolating roots; however, a different approach is implemented in TAHINI. First, the minima along the $\hat{\omega}_R$ -axis of $|D(\hat{\omega})|$, the modulus of the discriminant, are found. The values of $\hat{\omega}$ at these minima are then used as starting points in the application of a secant algorithm (e.g. Press et al. 1992) for convergence to roots of the discriminant in the complex- $\hat{\omega}$ plane;

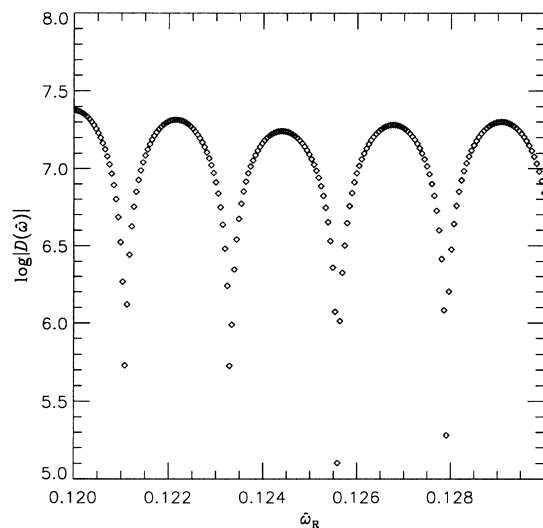


Figure 2. The modulus $|D(\hat{\omega})|$ of the discriminant as a function of $\hat{\omega}_R$, the real part of the dimensionless pulsation frequency $\hat{\omega}$. Local minima indicate the approximate location of eigenfrequencies in the complex- $\hat{\omega}$ plane.

the secant algorithm was chosen because it is trivially adapted to complex variables (e.g. Castor 1971).

This approach works by locating the ‘valley floors’ (one-dimensional minima) of $|D(\hat{\omega})|$, and then following these floors in the complex- $\hat{\omega}$ plane towards the roots of $D(\hat{\omega})$ which correspond to eigenfrequencies. It broadly parallels the solution-matching procedure used in the Riccati shooting technique (see, e.g. Gautschy & Glatzel 1990, equation 4.13 plus accompanying text) for pulsation problems, although the underlying algorithms adopted in solving the pulsation equations themselves differ fundamentally. Fig. 2 shows $|D(\hat{\omega})|$ along a selected range of the $\hat{\omega}_R$ -axis, for $\tilde{l} = 4$ modes of the stellar model considered in Section 4; the minima which lead to the eigenfrequencies of each mode are immediately apparent.

Note that TAHINI adopts a golden-section algorithm to locate the minima. More sophisticated approaches, such as Brent’s inverse parabolic interpolation algorithm (Press et al. 1992), cannot be used, since they rely on the second-order continuity of dependent variables; this property is absent when complete trapping occurs, because the gradient of $|D(\hat{\omega})|$ is discontinuous across the minima.

3.3 Modal classification

A procedure to classify modes in a unique and complete manner, as well as being taxonomically useful, is important for the \tilde{l} -track technique to function reliably. Sometimes, in the calculation of tracks, the relaxation method erroneously converges to solutions which neighbour the one under consideration. Such ‘track-jumping’ is especially prone to occur when a pair of modes undergo an avoided crossing (Aizenman et al. 1977), and the eigenfrequencies of the modes become very close. Modal classification is a straightforward way of detecting automatically when track-jumping has arisen, permitting appropriate action to be taken.

A classification scheme suitable for fully trapped modes was presented by Scuflaire (1974) and Osaki (1975), which consists of considering the so-called ‘phase path’ of solutions in the (ν, w) plane, where the phase variables ν and w are calculated from

eigenfunctions $y_{1,2}$ using

$$v = \frac{(\rho g r)^{1/2}}{|\lambda_{lm}/(c_1 \hat{\omega}^2) - V_g|^{1/2}} r^2 y_1 \quad (31)$$

and

$$w = \frac{(\rho g r)^{1/2}}{|c_1 \hat{\omega}^2 - A^*|^{1/2}} r^2 y_2; \quad (32)$$

these definitions have been adapted, for use within the tradition approximation, from the equivalent zero-rotation ones (e.g. Shibahashi 1979) through the usual trivial replacement of $l(l+1)$ with λ_{lm} . By following the phase path corresponding to a pair of eigenfunctions $y_{1,2}$ from the origin to the surface, the number of clockwise and anti-clockwise crossings of the axis $v = 0$ are enumerated. Denoting these two integers by N_p and N_g , respectively, their difference

$$\tilde{n} = N_p - N_g, \quad (33)$$

may be used as an unambiguous index, conserved during evolutionary changes to the stellar structure (Osaki 1975) and over changes in the harmonic degree l (Aizenman et al. 1977), for labelling each mode of a star. In unevolved stellar models, positive and negative \tilde{n} correspond to p - and g modes, respectively, whilst $\tilde{n} = 0$ corresponds to the f -mode.

This scheme requires modification in order to function properly when the leaky outer mechanical boundary condition (21) is adopted. Whilst the phase variables v and w are real, the eigenfunctions $y_{1,2}$ can be complex owing to leakage; therefore, it is pertinent to use the real parts of the latter when calculating phase paths via equations (31) and (32). This trivial adjustment corresponds to considering phase paths at a specific, but arbitrary, temporal phase.

A more-significant modification is necessary to deal with the influence of the leaky boundary condition on the terminal ($x = 1$) point of phase paths. Osaki (1975) adopted the zero boundary condition (14) throughout, so that y_1 and y_2 always agree in sign at the surface, and the terminal point is invariably located in the first ($v, w > 0$) or third ($v, w < 0$) quadrants of the (v, w) plane. However, when the leaky boundary condition is used, it is possible for the surface values of y_1 and y_2 to be opposite in sign, and for this terminal point to fall in the second ($-v, w > 0$) or fourth ($-v, w < 0$) quadrants of the plane. In such situations, the classification scheme discussed above sometimes leads to values of N_g which are smaller by unity than those anticipated, and the utility of \tilde{n} as an unambiguous modal index is compromised.

The reasons for the difficulty seem to lie in the assumption of wave evanescence at the surface, implicit in Osaki's (1975) adoption of the zero boundary condition; evidently, this assumption is violated when leakage occurs. However, surface evanescence can be artificially maintained by extending phase paths beyond the outer boundary with a supplementary phase segment; this segment, which follows a hyperbolic trajectory with asymptotic lines $w = \pm v$, characteristic of evanescent waves (see, e.g. Unno et al. 1989), is chosen to carry the the terminal point of the phase path into the first or third quadrant of the (v, w) plane. Fig. 3 illustrates the nature of typical supplementary segments, for eigenfunctions which lie, at the surface, in the second or fourth quadrants of the plane.

Adopting extended phase paths in the calculation of N_p and N_g (in the usual manner) was found to resolve the difficulty discussed above, for all modes apart from those with eigenfrequencies very

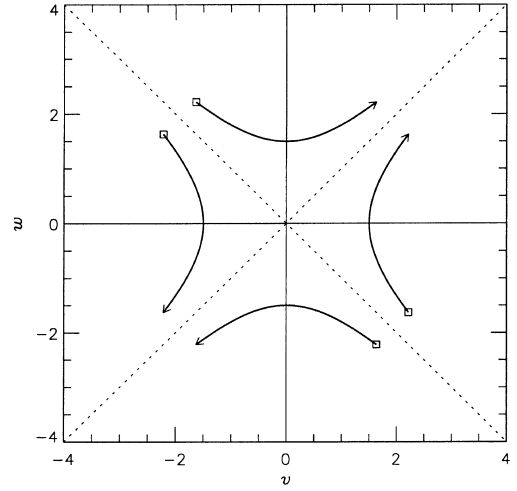


Figure 3. Typical supplementary phase-path segments in the (v, w) plane; these segments start at points corresponding to the outer boundary (squares), and follow hyperbolic trajectories (arrows) into the first or third quadrants of the plane. The dotted lines indicate the $w = \pm v$ asymptotic lines of the trajectories.

close to the trapping cut-off $\hat{\omega}_{c_1}$. The differential equations governing v and w (Unno et al. 1989) exhibit a turning point near the outer boundary for such modes; as a consequence, the asymptotic lines of evanescent-wave trajectories deviate from $w = \pm v$, and supplementary segments based on these lines may be incorrect. A heuristic yet effective solution to the problem is to adopt the asymptotes $w = \pm v/(1 + \epsilon)$ throughout the consideration of *all* supplementary segments, where $\epsilon \ll 1$ is a parameter which accounts for these deviations.

The actual calculation of supplementary segments is not necessary for implementation of the modified classification scheme. Instead, the value of N_g , calculated from the *original* phase path, is incremented by unity whenever the sign of v and w differ and $|w| > |v|/(1 + \epsilon)$ at the terminal point of the path; the value of N_p is left unaltered. This approach, which is functionally identical to adopting extended phase paths (but certainly less transparent), was implemented within TAHINI using an empirically determined value of 2×10^{-3} for the parameter ϵ . Prior to classification, all eigenfunctions $y_{1,2}$ are renormalized by TAHINI, such that $y_1 = 1$ at the inner boundary; this is to ensure that phase paths start in the first quadrant of the (v, w) plane, in accordance with the original prescription of Osaki (1975).

In its totality, the modified classification scheme implemented by TAHINI leads to a self-consistent and complete set of indices \tilde{n} for all modes considered throughout this work. As indicated at the start of this section, these indices are primarily used to detect automatically any track-jumping over an increment in \tilde{l} , during the calculation of \tilde{l} -tracks. When a discontinuity in \tilde{n} arises, indicative of a track-jump, TAHINI bisects the $\Delta\tilde{l}$ interval recursively, and the relaxation algorithm is applied over each resulting sub-interval, until the full interval can be traversed correctly.

4 RESULTS

In this section, results calculated using TAHINI are presented. The equilibrium stellar model adopted throughout is based on the same $7M_{\odot}$ ZAMS model of Paper I (see table 1 therein for the parameters of the star). Originally, this model consisted of 800

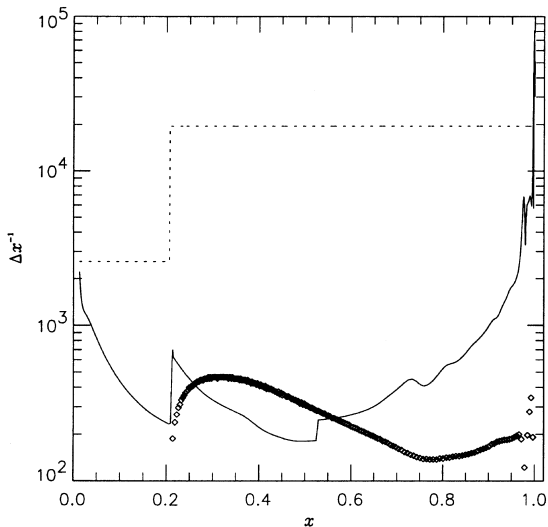


Figure 4. The grid density Δx^{-1} , where Δx is the spacing of adjacent grid points, as a function of normalized radius x , for the original (solid) and re-gridded (dotted) 7- M_{\odot} model. Also shown (diamonds) is the density of nodes of the highest-order (g_{210}) mode considered subsequently.

unequally distributed grid points extending from near the origin out to the surface at $x = 1$. For the calculations, it was necessary to re-grid the model, to ensure adequate resolution of the spatial oscillation of eigenfunctions in propagative regions; the new grid consisted of 15 500 and 500 uniformly distributed points in the envelope ($x \geq 0.2$) and core ($x \leq 0.2$) regions, respectively, the lower resolution in the core reflecting the fact that pulsation is invariably evanescent there owing to convection. Cubic spline interpolation (Press et al. 1992) was used to calculate quantities on the new grid. Denoting the spacing between adjacent grid points by Δx , Fig. 4 shows the grid density Δx^{-1} as a function of x for the original and re-gridded models. Also shown in the figure is the density of nodes ($y_1(x) = 0$) for the highest-order (g_{210}) mode considered subsequently; this nodal density is the effective Nyquist frequency required for minimal resolution of the spatial oscillations of the eigenfunction. Evidently, whilst the original model is woefully inadequate in the inner envelope ($0.25 \leq x \leq 0.55$), the re-gridded model provides good resolution of the eigenfunction, oversampling it by at least 40 times this effective Nyquist frequency.

4.1 \tilde{l} -tracks

All modes of the re-gridded 7- M_{\odot} model with eigenfrequencies in the interval $0.01 < \hat{\omega}_R < 2.5$ were found by TAHINI at $\tilde{l} = \tilde{l}_s = 1$, using the procedure discussed in Section 3.1. The modes, classified using the scheme presented in Section 3.3 as $g_{(-\tilde{n})} = g_{1 \dots g_{210}}$, were adopted by TAHINI as initial solutions in the calculation of corresponding \tilde{l} -tracks over the range $1 < \tilde{l} < 50$, at intervals $\Delta \tilde{l} = 0.05$; at every stage, the criterion applied for convergence of the relaxation method was that the fractional change in $|\hat{\omega}|$ over a single iteration did not exceed 10^{-9} .

The resulting tracks for the first 80 modes (i.e. $g_{1 \dots g_{80}}$) are displayed in Fig. 5. Rather than showing $\hat{\omega}$ itself, $\lambda_{lm}^{1/2}/\hat{\omega}_R$ is plotted in the figure. This latter quantity is approximately independent of \tilde{l} for a given mode in the asymptotic limit (see Lee & Saio 1987a; equation 23 of Paper I), and is a monotonically increasing function of the mode order $|\tilde{n}|$, so that the higher-order

modes appear towards the top of the figure. The imaginary part $\hat{\omega}_I$ of the eigenfrequency is not shown directly; however, different line styles are used to distinguish between trapped ($\hat{\omega}_I = 0$) and leaking ($\hat{\omega}_I > 0$) solutions. The tracks in the figure may be interpreted in one of two ways. At integral values of \tilde{l} , the frequencies corresponding to the track curves are identical to those of a non-rotating star pulsating with harmonic degree $l = \tilde{l}$. For more general (non-integral) values of \tilde{l} , however, these frequencies are pertinent to a rotating star pulsating with $\lambda_{lm} = \tilde{l}(\tilde{l} + 1)$.

The outstanding feature of the figure is the discrete nature of the eigenfrequency spectrum, even after the onset of wave leakage at $\lambda_{lm}^{1/2}/\hat{\omega}_R \approx 38.5$ (see also Fig. 2). In Paper I, it was implied that this phenomenon was a consequence of the convection zone at $\log T \approx 4.6$, owing to He II ionization, which acts as a partially reflecting barrier to waves incident from the interior. However, when the zone was artificially eliminated by modifying the values of A^* (equation 5) across its extent, it was found that the discrete character of the spectrum remained. An alternative explanation has been given by Gautschy (1992), who considered the related problem of leaking p -modes in Ap stars. He argued that such modes will be discrete because of a combination of the complete reflection of waves at the stellar origin, and the assumption that only outwardly propagating waves are present at the stellar surface.

The same reasoning can be used to explain the discrete character of the virtual (leaking) g modes considered herein: the leaky boundary condition (21) automatically pre-selects only outgoing waves, and complete reflection of waves at the origin is assured by the fact that the Brunt–Väisälä frequency is zero there. Evidently, then, the convection zone is not important in generating the discrete nature of the mode spectrum; however, as will be demonstrated in Section 4.3, it does play a rôle in controlling the degree of damping as a result of leakage.

At $\tilde{l} = 1$, the $g_{53 \dots g_{80}}$ modes are virtual, whilst the $g_1 \dots g_{52}$ modes are fully trapped. As \tilde{l} is increased, it is evident from inspection of Fig. 5 that some of the latter undergo a transition to virtual modes and begin to leak; this occurs first for the g_{52} mode at $\tilde{l} \approx 17.5$, then for the g_{51} mode at $\tilde{l} \approx 25.5$, and so on. The transition is primarily the result of the departure of eigenfrequencies from the asymptotic limit, which manifests itself in the gradual increase of $\lambda_{lm}^{1/2}/\hat{\omega}_R$ with \tilde{l} . This limit holds only for the higher-order modes at small values of \tilde{l} , which exhibit tracks which appear almost horizontal. The existence of such a transition apparently invalidates the hypothesis, suggested in Paper I, that the set of modes trapped within a star is invariant under the influence of rotation.

One other feature in the figure which warrants brief discussion is the appearance of avoided crossings between trapped-mode tracks at $\tilde{l} \approx 33.5$ (g_7 and g_8) and $\tilde{l} \approx 44.5$ (g_6 and g_7). Avoided crossings usually arise when modes are trapped within two well-separated regions of the star (e.g. Osaki 1975); in the present case, these regions are identified as the inner envelope, and the outer part of the He II convection zone. In the former and the latter, waves have the character of g - and p -modes, respectively, as can be seen from the propagation diagrams presented in Paper I; therefore, the avoided crossings indicate the presence of mixed-character modes.

4.2 Eigenfrequencies

The mapping procedure discussed in Section 3.1 was applied to

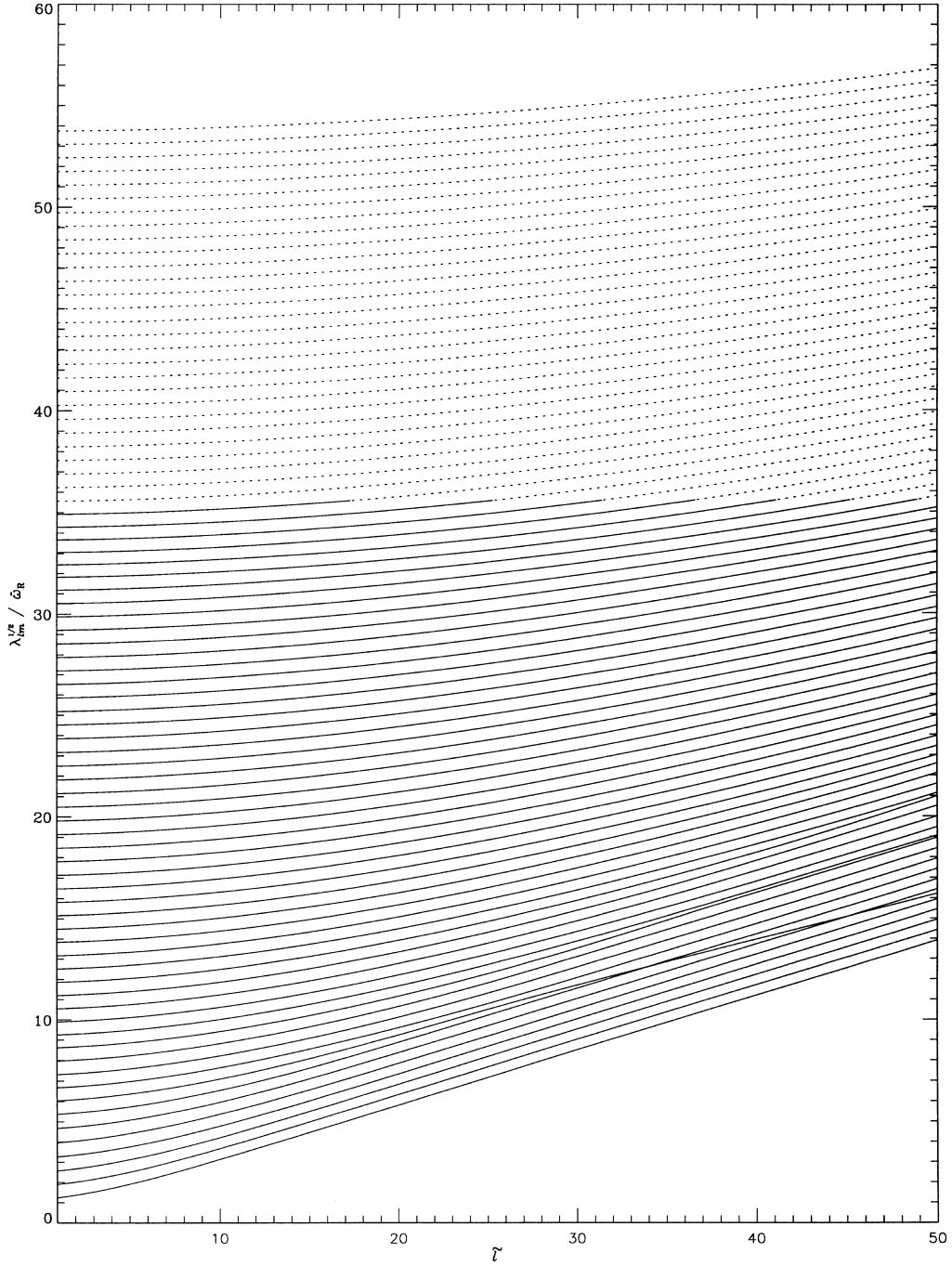


Figure 5. \tilde{l} -tracks for the $g_1 \dots g_{80}$ modes of the $7-M_{\odot}$ model, shown by plotting $\lambda_{lm}^{1/2}/\hat{\omega}_R$ as a function of \tilde{l} . Solid and dotted lines indicate trapped and virtual (leaking) modes, respectively.

the \tilde{l} -tracks calculated previously, to find the dependence of $\hat{\omega}_R$ on Ω for all $l = 4$ pulsation modes apart from the zonal ($m = 0$) mode, the latter generally being unimportant as a source of line-profile variability. The eigenvalue λ_{lm} was tabulated, using the same method as in Paper I, at 1000 points uniformly sampling the range $0 \leq \nu \leq 5$ for the $m = 1$ modes, $0 \leq \nu \leq 30$ for the $m = -4$ modes, and $0 \leq \nu \leq 7$ for all other modes; these upper limits on ν ensured adequate final coverage of Ω . Interpolation of $\hat{\omega}_R$ in \tilde{l} -tracks was performed using cubic splines. The resulting eigenfrequencies (or, rather, the real parts $\hat{\omega}_R$) are shown in Fig. 6 as a function of the parameter $\Omega/\Omega_{\text{crit}}$, where the dimensionless

critical rotation rate Ω_{crit} is defined by

$$\Omega_{\text{crit}}^2 = \frac{8GM}{27R^3}. \quad (34)$$

The upper limit $\Omega/\Omega_{\text{crit}} = 0.75$ displayed in the figure was chosen to reflect the fact that, as Ω approaches Ω_{crit} , centrifugal-force effects neglected within the traditional approximation begin to have a significant effect on the stellar geometry and cannot be disregarded. Note that, in order to improve the clarity of the figure, only the odd- \tilde{n} (i.e. $g_1, g_3, g_5 \dots g_{77}, g_{79}$) modes are shown.

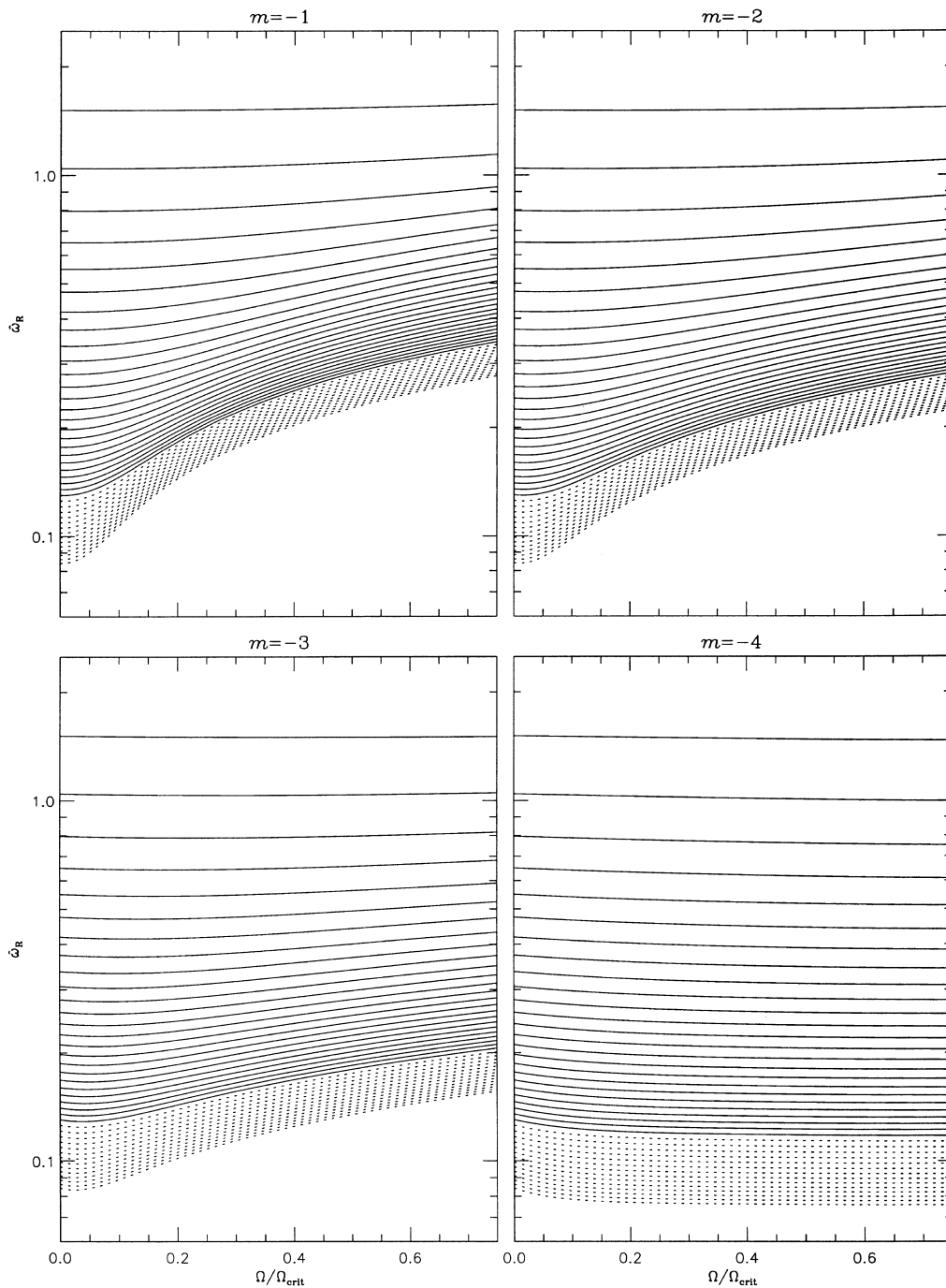


Figure 6. The real part $\hat{\omega}_R$ of the eigenfrequency for prograde $m < 0$, $l = 4$, odd- \tilde{n} g modes of the $7-M_\odot$ model, plotted as a function of $\Omega/\Omega_{\text{crit}}$. Solid and dotted lines indicate trapped and virtual (leaking) modes, respectively. As before, except that the retrograde $m > 0$ modes are shown.

As with Fig. 5, each panel of this figure shows a pronounced division between trapped and virtual modes, which here can be identified with the trapping cut-off $\hat{\omega}_{c_1}$. The figure confirms the qualitative findings of Paper I, namely, that the effect of rotation is to increase $\hat{\omega}_{c_1}$ for all but the prograde sectoral modes; furthermore, this increase is most pronounced for the retrograde ($m > 0$) modes, and those for which $(l - |m|)$ is largest. The notable exceptions to this behaviour are the prograde sectoral modes, for which $\hat{\omega}_{c_1}$ decreases monotonically with increasing rotation rate, owing to the transformation of the modes into equatorially trapped Kelvin waves (Paper I). Note that, as Ω is

gradually increased from zero, $\hat{\omega}_{c_1}$ first decreases for *all* prograde modes; this occurs because $d\lambda_{lm}/d\nu < 0$ at $\nu = 0$ when $m < 0$ (Lee & Saio 1997).

These points apply not only to the cut-off $\hat{\omega}_{c_1}$, but also to the mode eigenfrequencies themselves (or, more specifically, the real parts $\hat{\omega}_R$). The effects of rotation are most pronounced for the high-order modes, since the Coriolis force has the greatest influence on slow, long time-scale waves; as a consequence, the density of the mode spectrum increases with Ω for all but the prograde sectoral modes. This result raises questions regarding the self-excitation of single, small- $l|m|$ and/or retrograde pulsation modes

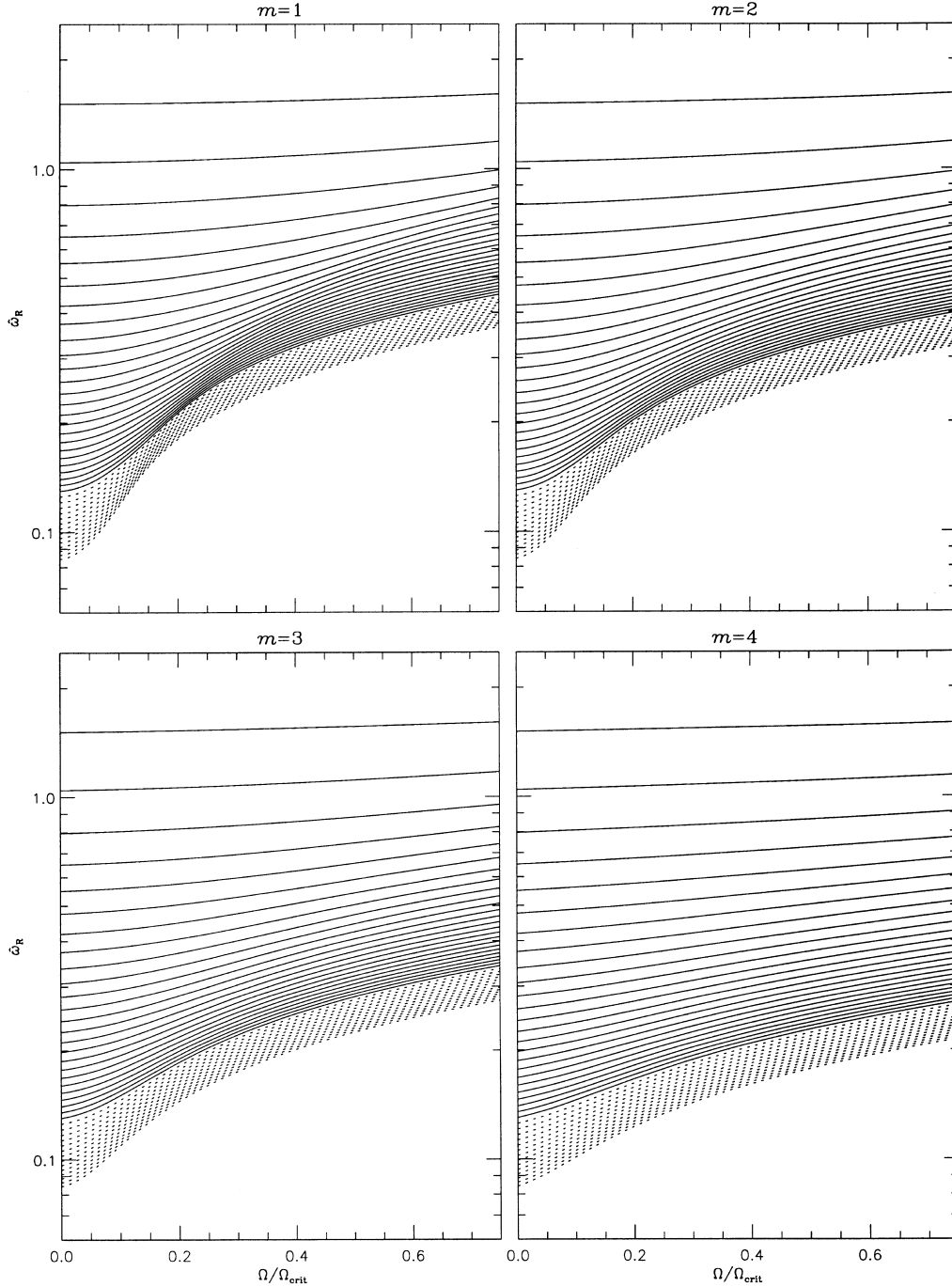


Figure 6 – continued

in rapidly rotating stars (e.g. Be stars), since these systems will possess exceedingly dense mode spectra, and it is not clear what kind of mechanism could lead to the selective excitation of one mode, without simultaneously exciting neighbouring ones.

Unlike the \tilde{l} -tracks shown in Fig. 5, no trapped modes become virtual over the range of Ω displayed in Fig. 6. This is because, for the $l = 4$ modes, \tilde{l} never becomes large enough (≥ 17.5) for a transition from trapped to virtual to occur. Therefore, whilst the hypothesis of rotation-invariant trapping is formally invalidated by Fig. 5, it may well be the case that it holds in all physically relevant situations.

4.3 Damping rates

As discussed previously, the outward loss of mechanical wave energy through the stellar surface causes the amplitude of virtual modes to decay with time. The strength of such ‘advective damping’ (see Paper I) is characterized by

$$\eta_d \equiv \frac{\hat{\omega}_I}{\hat{\omega}_R}, \quad (35)$$

such that the fractional change in the amplitude of a mode, over one pulsation cycle, is given by $\exp(-2\pi\eta_d)$. When $\hat{\omega}_I \ll \hat{\omega}_R$,

this advective damping rate η_d is related to the work integral W (e.g. Ando & Osaki 1975) of the pulsation through

$$\eta_d = -\frac{1}{4\pi} \frac{W}{E_T}, \quad (36)$$

where E_T , the time-averaged total pulsation energy of the star, is given in terms of the fluid displacement vector ξ as

$$E_T = \int_0^M \langle \mathcal{E} \rangle dM_r = \frac{\omega_R^2}{2} \int_0^M |\xi|^2 dM_r. \quad (37)$$

The work integral is a measure of the increase in E_T over one pulsation cycle, and may be written in the form (Unno et al. 1989)

$$W = \oint dt \left(\int_0^M \delta T \frac{d\delta S}{dt} dM_r - \oint_S \mathbf{F}_W \cdot d\mathbf{A} \right), \quad (38)$$

where δT and δS are the Lagrangian perturbations to the temperature and specific entropy, respectively, \mathbf{F}_W is the mechanical energy flux discussed in Section 2.2, $d\mathbf{A}$ is the vector surface-area infinitesimal and S is the surface of the star. In the present case, the first term in this expression is identically zero, since $\delta S = 0$ in

the adiabatic approximation. Thus,

$$W = -\oint dt \oint_S \mathbf{F}_W \cdot d\mathbf{A} = -\frac{\omega_R}{2\pi} \oint_S \langle \mathbf{F}_W \rangle \cdot d\mathbf{A}, \quad (39)$$

in combination with (36), indicates that η_d is proportional to the time-averaged outward flux of wave energy owing to leakage.

Fig. 7 shows η_d as a function of $\hat{\omega}_R$ for the $l=4$, $m=1$ g modes of the 7- M_\odot model; unlike the preceding section, both odd- and even- \tilde{n} modes are shown, in order to illustrate fully the dependence of η_d on $\hat{\omega}_R$. The division between trapped ($\eta_d = 0$) and virtual ($\eta_d > 0$) modes is immediately apparent, as is the increase in the trapping cut-off $\hat{\omega}_{c_1}$ with Ω . The order of magnitude of η_d for the virtual modes ($\sim 10^{-4}$), which was found to be similar for other values of l and m , supports a posteriori the validity of adopting the steady-wave approximation introduced in Section 3.1. The implications of this value, with regards to the self-excitation of virtual modes, are discussed below in Section 5.

The repetitive structure of η_d , evident in every panel of the figure, can be attributed to the differing energy distribution of each virtual mode. For such modes, the star is divided into two propagative regions by the He II convection zone at $\log T \approx 4.6$

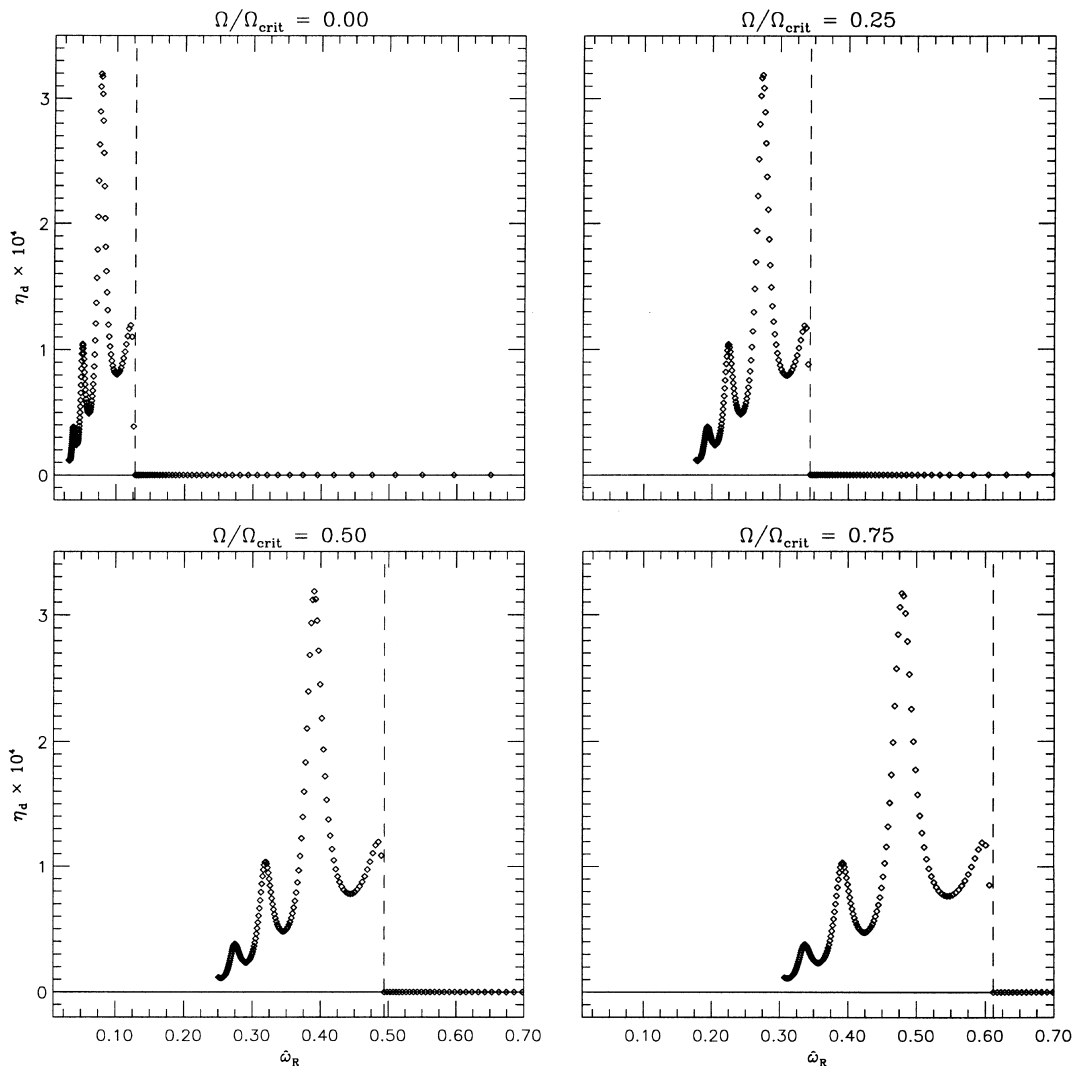


Figure 7. The damping rate η_d , as a function of the real part $\hat{\omega}_R$ of the eigenfrequency, for $l=4$, $m=-1$ g modes of the 7- M_\odot model, at four selected rotation rates. The dashed vertical line shows the location of the trapping cut-off $\hat{\omega}_{c_1}$.

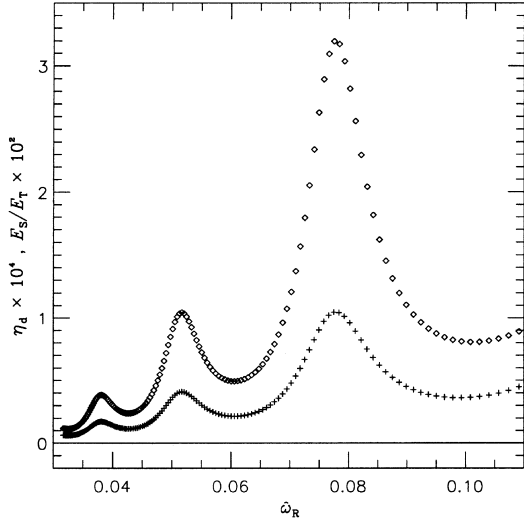


Figure 8. The partition measure E_S/E_T (crosses) and the damping rate η_d (diamonds) as a function of $\hat{\omega}_R$, for $l = 4$ g modes of the 7- M_\odot model in the zero-rotation limit.

(see figs 1 and 2 of Paper I), and the total energy E_T may be partitioned into contributions from each of these regions. Let M_i denote the mass interior to the outer boundary of the zone; then

$$E_S = \frac{\omega_R^2}{2} \int_{M_i}^M |\xi|^2 dM_r \quad (40)$$

is the contribution to the total energy from the surface regions above the convective zone, and the ‘partition measure’ E_S/E_T is an indication of the relative significance of these regions in the pulsation energy distribution. Fig. 8 shows the latter values plotted over the corresponding damping rates taken from the zero-rotation panel of Fig. 7.

Evidently, there is a direct correlation between the two quantities, which is easily explained. As indicated in Section 4.1, the convection zone behaves like a partially reflecting barrier to waves incident from the interior, which tends to restrict the leakage of mechanical energy from the star. Those virtual modes with the larger partition measures are (energetically) relatively concentrated in regions above the barrier, and do not benefit so much from its influence as a leakage ‘throttle’. Therefore, the damping rate associated with such modes is correspondingly greater, as is apparent in the figure.

The underlying decrease in both η_d and the partition measure, as $\hat{\omega}_R$ is lowered, arises from the evanescent character of virtual g modes across the He II convection zone. Within the zone, the eigenfunctions of these modes will vary as

$$y_{1,2} \sim \exp(ik_r r), \quad (41)$$

where the radial wavenumber k_r is given in the low-frequency limit, from a local analysis (Paper I), by

$$k_r \sim \frac{\sqrt{\Lambda_{lm}}}{\omega r} N. \quad (42)$$

Across the zone, N^2 is negative, and k_r will be imaginary, so that the eigenfunctions decay exponentially with a scale height proportional to ω . Evidently, then, the effectiveness of the zone as a leakage throttle increases as the frequency is lowered, which

explains the corresponding decline in both the damping rate and the partition measure.

4.4 Surface perturbations

In addition to providing a necessary constraint for solution of the pulsation equations, the outer mechanical boundary condition dictates the nature of pulsation at the stellar surface, and is of paramount importance in determining the pulsation-originated line-profile variations (lpv) exhibited by a star. The principal sources of such variability in rapidly rotating early-type stars are velocity and temperature perturbations to photospheric fluid elements (e.g. Townsend 1997b). The former may be expressed in spherical polar co-ordinates as

$$\mathbf{v} = i\omega \left(y_1, \frac{y_2}{\hat{\omega}^2} \nabla_\theta^\nu, \frac{y_2}{\hat{\omega}^2} \nabla_\phi^\nu \right) \Theta_l^m(\mu; \nu) \exp[i(m\phi + \omega t)], \quad (43)$$

where the operators ∇_θ^ν and ∇_ϕ^ν , defined by

$$\nabla_\theta^\nu = \frac{1}{(1 - \mu^2 \nu^2) \sqrt{1 - \mu^2}} \left[-(1 - \mu^2) \frac{d}{d\mu} + m\nu\mu \right], \quad (44)$$

$$\nabla_\phi^\nu = \frac{i}{(1 - \mu^2 \nu^2) \sqrt{1 - \mu^2}} \left[-\nu\mu(1 - \mu^2) \frac{d}{d\mu} + m \right], \quad (45)$$

may be regarded as rotationally modified equivalents to the latitudinal and azimuthal components, respectively, of the spherical-polar gradient operator. Within the adiabatic approximation, the Lagrangian temperature perturbation δT is proportional to the Lagrangian pressure perturbation δp ; equation (13) then gives

$$\frac{\delta T}{T} = \nabla_{\text{ad}} V(y_2 - y_1) \Theta_l^m(\mu; \nu) \exp[i(m\phi + \omega t)], \quad (46)$$

where ∇_{ad} is the adiabatic temperature gradient at the stellar surface. These expressions demonstrate that the characteristics of photospheric perturbations are dependent on the relative amplitudes and phases of the eigenfunctions $y_{1,2}$ at the surface; the latter are, in turn, determined by the choice of outer mechanical boundary condition.

Previous attempts at modelling the lpv of early-type stars (e.g. Vogt & Penrod 1983; Gies 1991; Aerts & Waelkens 1993; Telting & Schrijvers 1997; Townsend 1997a,b) have typically used the zero boundary condition (14) in the evaluation of velocity fields (43), and, where appropriate, the expression given by Buta & Smith (1979) for calculating temperature perturbations; the latter may be derived by substituting the boundary condition introduced by Dziembowski (1971) into equation (46). Such approaches have been fairly successful in reproducing the qualitative features of lpv; however, they have met with difficulty in modelling correctly the distribution of variability power across a given line profile, which might be the result of a lack of physical sophistication in the boundary conditions adopted for calculations.

Whilst proper lpv modelling, in the context of wave leakage, is deferred to the following paper in this series, it is pertinent to examine the differences between the three outer mechanical boundary condition formulations (equations 14, 15 and 21). Fig. 9 shows the modulus and argument of the surface value of y_2 for the $l = 4$ g modes considered in the previous section, calculated using the normalization (12) and the leaky boundary condition (21) in the zero-rotation limit. Also shown are the corresponding values which would result from adopting the zero boundary condition (14) and Dziembowski’s boundary condition (15). Although there is little to distinguish between the three at higher frequencies,

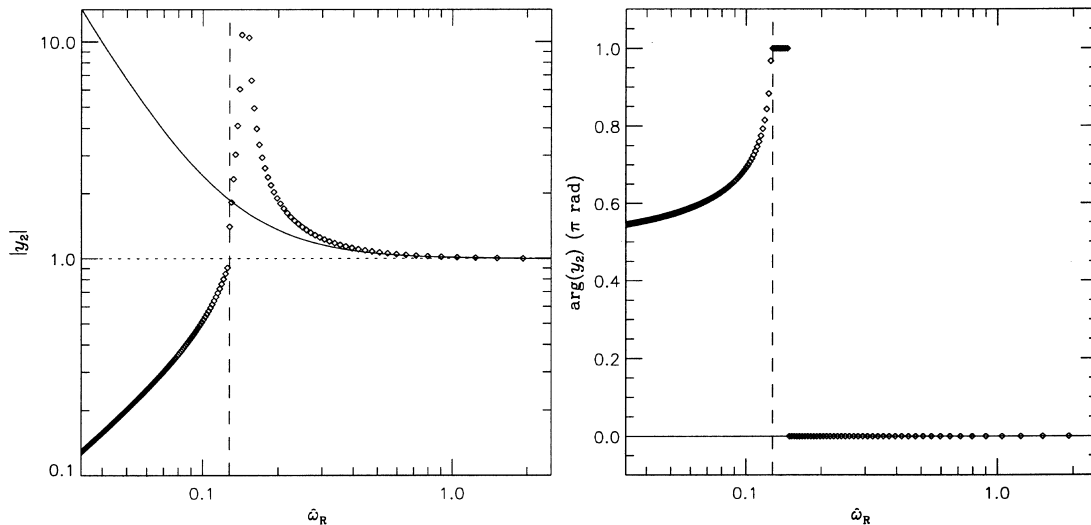


Figure 9. The modulus and argument of the surface value of y_2 , as a function of $\hat{\omega}_R$ for $l = 4$ g modes of the $7-M_\odot$ model in the zero-rotation limit. Diamonds show modes calculated using the leaky boundary condition (21), whilst solid and dotted lines show the corresponding values calculated using the zero boundary condition (14) and Dziembowski’s boundary condition (15), respectively. The dashed vertical line shows the location of the trapping cut-off $\hat{\omega}_{c_1}$.

marked differences between each are apparent for lower-frequency modes. Most significantly, the leaky boundary condition predicts a phase difference between y_1 and y_2 , approaching $\pi/2$ rad in the limit $\hat{\omega}_R \ll \hat{\omega}_{c_1}$; this is in contrast to the other two boundary conditions, which indicate that y_1 and y_2 remain in phase for all $\hat{\omega}_R$.

The other important difference between the three boundary conditions is the predicted amplitude of y_2 , relative to y_1 . At frequencies below the trapping cut-off, this amplitude is significantly smaller when calculated using the leaky boundary condition, than when using the other two. Since the strength of horizontal velocity fields is proportional to y_2 via equation (43), this may be of relevance in resolving the so-called ‘K-problem’ (e.g. Smith 1980, 1982, 1986), where observations of lpv in some stars suggest horizontal velocity fields much smaller than those predicted by theory. Similarly, the accompanying change in temperature perturbations may help to explain discrepancies between photometric and spectroscopic pulsation amplitudes (e.g. Buta & Smith 1979; Smith & Buta 1979). These issues are examined in greater detail in the following paper.

5 DISCUSSION

As with Paper I, a caveat regarding the qualitative interpretation of the results presented herein must be stipulated: the atmospheric layers above the photosphere have been neglected in calculations. Waves which leak from the star may subsequently be reflected by these layers, invalidating the assumption that no inwardly propagating wave component is present at the outer boundary. However, as before, the results remain valid on a phenomenological level, and in the present case serve to confirm, via a more-rigorous global analysis, the principal assertions of Paper I:

- (i) wave leakage occurs at frequencies below some trapping cut-off,
- (ii) the eigenfrequency spectrum remains discrete at frequencies below the cut-off, and
- (iii) the cut-off is significantly increased by the action of the Coriolis force, for all but the prograde sectoral modes.

Note, however, that (ii) occurs for the reasons discussed by Gautschy (1992), rather than those suggested in Paper I (see Section 4.1). The results also indicate that, formally, the hypothesis of rotation-invariant trapping proposed in Paper I is incorrect; however, it may be the case that the hypothesis holds in all physically significant scenarios.

The interplay between non-adiabatic excitation and damping mechanisms, and advective damping owing to wave leakage, determines whether a given mode will be overstable in a star. Dziembowski et al. (1993) have demonstrated that a metal-opacity bump at $\log T \approx 5.3$ is probably responsible for the excitation of higher-order g modes in the 53 Per (Smith 1977) and SPB (Waelkens 1991) variable stars; however, these stability calculations used the outer mechanical boundary condition introduced by Dziembowski (1971), which implicitly enforces complete wave trapping at the stellar surface, and thus neglects the effects of advective damping. In spite of this point, it is unlikely that the latter will have any significant influence on which modes are unstable in a star, for the reason given in Paper I: radiative damping will probably stabilize modes well before the pulsation frequency is low enough for leakage to occur.

In support of this conclusion, Dziembowski et al. (1993) found, for instance, that $l = 4$ g modes in a (non-rotating) $4-M_\odot$ model star were overstable to the opacity mechanism only up to a limiting value ($\bar{n} \approx 40$) of the radial order; higher-order modes were not excited, as a result of the dominance of radiative damping. This upper limit is significantly smaller than the lower limit ($\bar{n} \approx 53$) found in Section 4.1 for the onset of wave leakage; whilst a direct comparison of these two figures is not rigorous, it would appear that all g modes found to be overstable by Dziembowski et al. (1993) will be fully trapped, and, as a corollary, that no virtual mode excitation will occur in the stars they considered. Nevertheless, the adoption of the leaky boundary condition (21) may still influence the stability of the fully trapped modes, owing to the fact that surface values of y_2 , relative to y_1 , differ from those predicted by Dziembowski’s (1971) boundary condition (see Fig. 9).

An interesting phenomenon discussed by Wang et al. (1995) warrants mention at this point. They found that the trapping

cut-off frequencies for vertical wave propagation in an isothermal atmosphere are only well defined when the wave amplitude is time independent. In other situations, when the amplitude grows or decays exponentially with time, leakage will occur at all frequencies, and, formally, no trapping cut-offs exist. The same result is evident from inspection of Fig. 1: the propagation discriminant ψ is complex, and waves are propagative at the surface via equation (23), whenever $\hat{\omega}_1$ is non-zero. Therefore, if non-adiabatic effects are included, such that $\hat{\omega}$ is always complex, leakage will occur even for those ‘trapped’ g modes whose eigenfrequencies lie *above* the formal low-frequency cut-off; however, the degree of this leakage is expected to be negligible.

As Dziembowski et al. (1993) stress, their calculations neglect the influence of rotation; therefore, the preceding conclusions regarding the non-excitation of virtual modes is appropriate only for the 53 Per stars, which by definition are narrow lined, and the slowly rotating SPB stars found in Waelkens’s (1991) original sample. Whilst some qualitative analyses of vibrational stability in rapidly rotating stars have been made (e.g. Osaki 1974; Lee & Saio 1987b; Lee & Baraffe 1995), few *quantitative* data are available; the overstability of virtual modes in these systems remains a possibility, and will depend, amongst other things, on the degree of advective damping arising from leakage. The latter was found in Section 4.3 to have an order of magnitude of 10^{-4} ; this value, which is dependent on the thickness of the subsurface He II convection zone, is appreciably larger than typical non-adiabatic growth rates ($\sim 10^{-5}$) found by Dziembowski et al. (1993) for opacity-driven pulsation. Evidently, if virtual modes are to be self-excited to observable amplitudes in rapidly rotating early-type stars, any putative excitation mechanism operative in these systems must be significantly more robust than those already known for the non-rotating stars. Reliable conclusions on this issue must await fully non-adiabatic calculations which include the effects of both rotation and leakage; such studies are planned for the near future.

On a final note, the reader may wonder why significant discussion has been devoted to the overstability of virtual modes. The reasons for this emphasis lie in the results presented in Section 4.4, in particular the predicted phase differences between y_1 and y_2 for these modes. As will be demonstrated in the following paper, such phase differences will lead to pronounced asymmetries in the lpv generated by surface velocity fields and temperature perturbations. Similar asymmetries have been observed in a number of rapidly rotating early-type stars (e.g. λ Eri – Gies 1994; HD64760 – Howarth et al. 1998; μ Cen – Rivinius et al., in preparation), and one motivation behind this series of papers is to examine whether such lpv morphologies can be explained in terms of wave leakage and self-excited virtual modes. In addition, wave leakage may play a role in explaining the Be phenomenon, by providing a source of energy and angular momentum for the observed episodic disc formation, and therefore definitely warrants investigation.

6 CONCLUSIONS

The results presented in this paper lead to conclusions similar to those drawn in Paper I, and serve to strengthen the latter by a more-rigorous global analysis. However, the fact that leakage only occurs when the radial order \bar{n} is suitably large (≥ 53) indicates that virtual modes will probably *not* be excited in 53 Per or slowly rotating SPB stars; nevertheless, the stability calculations of Dziembowski et al. (1993) and other authors for these stars may

still be influenced by the findings of this and the preceding paper, as a result of alterations to the outer mechanical boundary condition.

Whether virtual modes will be overstable in Be stars or the more rapidly rotating SPB stars (Aerts et al. 1999) depends on the existence of a putative excitation mechanism, which is significantly more robust than that known for the 53 Per and slowly rotating SPB stars; this result follows from the fact that damping rates owing to leakage are typically quite large. If such excitation does occur, the leaky outer mechanical boundary condition predicts significant modifications to the characteristics of surface velocity fields and temperature perturbations owing to the pulsation.

ACKNOWLEDGMENTS

I would like to thank Ian Howarth and Myron Smith for their helpful feedback on the paper, and especially Alfred Gautschy, for pointing me towards the explanation for the discrete character of leaking modes. This work has been supported by the Particle Physics and Astronomy Research Council of the UK.

REFERENCES

- Aerts C., Waelkens C., 1993, *A&A*, 273, 135
- Aerts C. et al., 1999, *A&A*, 343, 872
- Aizenman M. L., Smeyers P., 1977, *Ap&SS*, 48, 123
- Aizenman M. L., Smeyers P., Weigert A., 1977, *A&A*, 58, 41
- Ando H., 1983, *PASJ*, 35, 343
- Ando H., Osaki Y., 1975, *PASJ*, 27, 581
- Bildsten L., Ushomirsky G., Cutler C., 1996, *ApJ*, 460, 827
- Buta R. J., Smith M. A., 1979, *ApJ*, 232, 213
- Castor J. I., 1971, *ApJ*, 166, 109
- Cowling T. G., 1941, *MNRAS*, 101, 367
- Dziembowski W. A., 1971, *Acta Astron.*, 21, 290
- Dziembowski W. A., 1977, *Acta Astron.*, 27, 95
- Dziembowski W. A., Moskalik P., Pamyatnykh A. A., 1993, *MNRAS*, 265, 588
- Eckart C., 1960, *Hydrodynamics of Oceans and Atmospheres*. Pergamon Press, Oxford
- Gautschy A., 1992, *MNRAS*, 256, 11P
- Gautschy A., Glatzel W., 1990, 245, 154
- Gies D. R., 1991, in Baade D., eds, *Rapid Variability of OB-Stars: Nature and Diagnostic Value*. ESO, Munich, p. 229
- Gies D. R., 1994, in Balona L. A., Henrichs H. F., Le Contel J. M., eds, *Proc. IAU Symp. 162, Pulsation, Rotation and Mass Loss in Early-Type Stars*. Kluwer, Dordrecht
- Gill A. E., 1982, *Atmosphere-Ocean Dynamics*. Academic Press, London
- Glatzel W., Gautschy A., 1992, *MNRAS*, 256, 209
- Howarth I. D., Townsend R. H. D., Clayton M. J., Fullerton A. W., Gies D. R., Massa D., Prija R. K., Reid A. H. N., 1998, *MNRAS*, 296, 949
- Kippenhahn R., Weigert A., 1990, *Stellar Structure and Evolution*. Springer-Verlag, Berlin
- Lee U., Baraffe I., 1995, *A&A*, 301, 419
- Lee U., Saio H., 1987a, *MNRAS*, 224, 513
- Lee U., Saio H., 1987b, *MNRAS*, 225, 643
- Lee U., Saio H., 1989, *MNRAS*, 237, 875
- Lee U., Saio H., 1990, *ApJ*, 349, 570
- Lee U., Saio H., 1997, *ApJ*, 491, 839
- Osaki Y., 1974, *ApJ*, 189, 469
- Osaki Y., 1975, *PASJ*, 27, 237
- Osaki Y., Hansen C. J., 1973, *ApJ*, 185, 277
- Press W. H., Teukolsky S. A., Vetterling W. T., Flannery B. P., 1992, *Numerical Recipes in FORTRAN*. Cambridge Univ. Press, Cambridge
- Scuflaire R., 1974, *A&A*, 36, 107

- Shibahashi H., 1979, *PASJ*, 31, 87
 Shibahashi H., Osaki Y., 1981, *PASJ*, 33, 427
 Smith M. A., 1977, *ApJ*, 215, 574
 Smith M. A., 1980, in Hill H. A., Dziembowski W., eds, *Nonradial and Nonlinear Stellar Pulsation*. Springer Verlag, New York, p. 60
 Smith M. A., 1982, *ApJ*, 254, 708
 Smith M. A., 1986, in Osaki Y., eds, *Hydrodynamic and Magnetohydrodynamic Problems in the Sun and Stars*. Univ. Tokyo Press, Tokyo, p. 145
 Smith M. A., Huang L., 1994, in Balona L. A., Henrichs H. F., Le Contel J. M., eds, *Proc. IAU Symp. 162, Pulsation, Rotation and Mass Loss in Early-Type Stars*. Kluwer, Dordrecht
 Smith M. A., Buta R. J., 1979, *ApJ*, 232, L193
 Telting J. H., Schrijvers C., 1997, *A&A*, 317, 723
 Townsend R. H. D., 1997a, *MNRAS*, 284, 839
 Townsend R. H. D., 1997b, PhD thesis, Univ. London
 Townsend R. H. D., 2000, *MNRAS*, in press (Paper I)
 Unno W., Osaki Y., Ando H., Saio H., Shibahashi H., 1989, *Nonradial Oscillations of Stars*. Univ. Tokyo Press, Tokyo
 Vogt S. S., Penrod G. D., 1983, *ApJ*, 275, 661
 Waelkens C., 1991, *A&A*, 246, 453
 Wang Z., Ulrich R. K., Coroniti F. V., 1995, *ApJ*, 444, 879

This paper has been typeset from a \TeX/L\TeX file prepared by the author.